FLUID MECHANICS

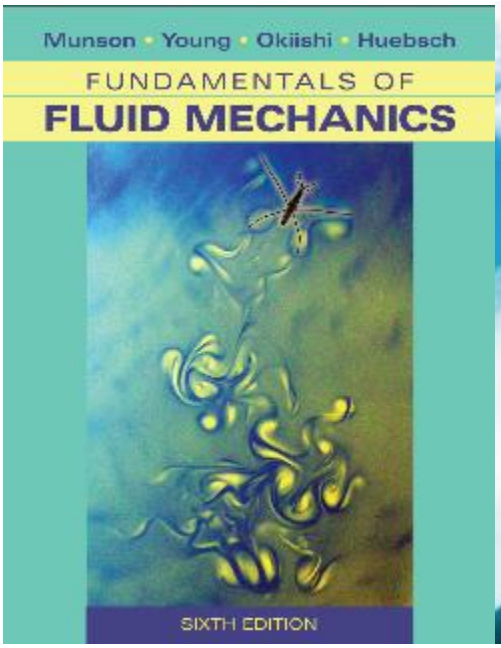

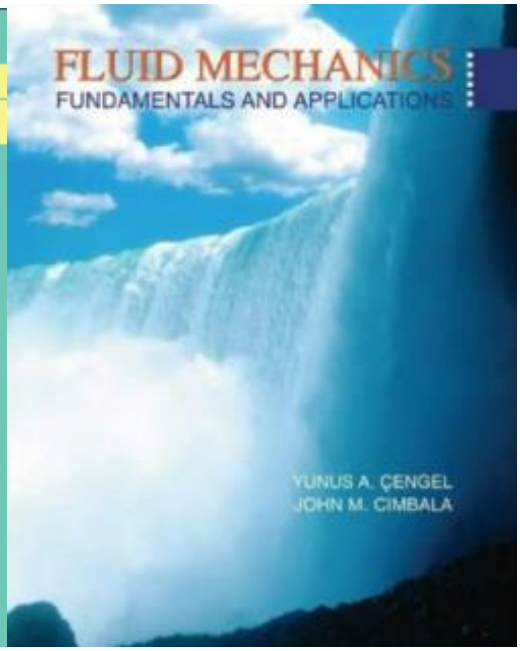

PROF. DR. METİN GÜNER
COMPILER

ANKARA UNIVERSITY
FACULTY OF AGRICULTURE
DEPARTMENT OF AGRICULTURAL MACHINERY AND TECHNOLOGIES ENGINEERING

5. FLOW IN PIPES

5.3. Fully Developed Turbulent Flow

Consider a long section of pipe that is initially filled with a fluid at rest. As the valve is opened to start the flow, the flow velocity and, hence, the Reynolds number increase from zero (no flow) to their maximum steady-state flow values, as is shown in Fig.5.10. Assume this transient process is slow enough so that unsteady effects are negligible (quasi-steady flow). For an initial time period the Reynolds number is small enough for laminar flow to occur. At some time the Reynolds number reaches 2100, and the flow begins its transition to turbulent conditions. Intermittent spots or bursts of turbulence appear. As the Reynolds number is increased, the entire flow field becomes turbulent. The flow remains turbulent as long as the Reynolds number exceeds approximately 4000.

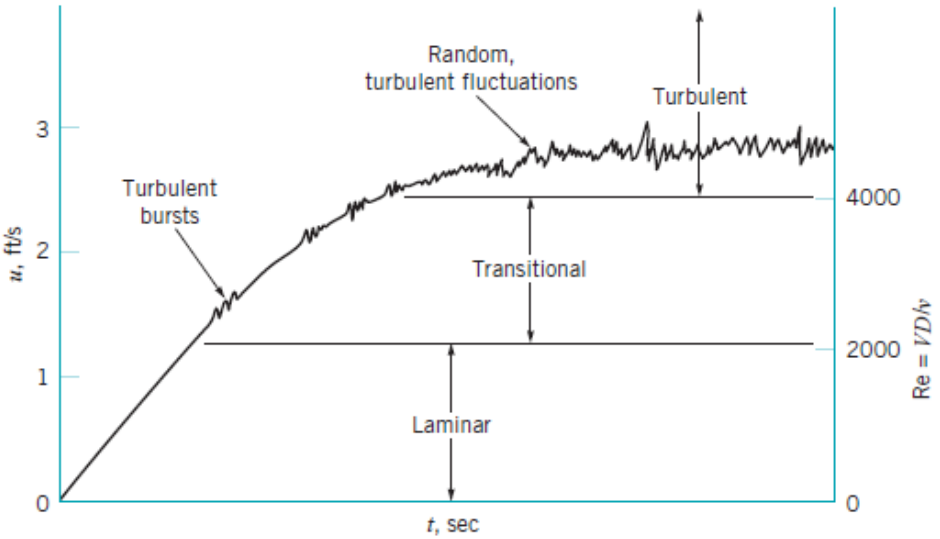

Figure 5.10. Transition from laminar to turbulent flow in a pipe.

A typical trace of the axial component of velocity measured at a given location in the flow, u=u(t), is shown in Fig.5.11. Its irregular, random nature is the distinguishing feature of turbulent flow. The character of many of the important properties of the flow (pressure drop, heat transfer, etc.) depends strongly on the existence and nature of the turbulent fluctuations or randomness indicated.

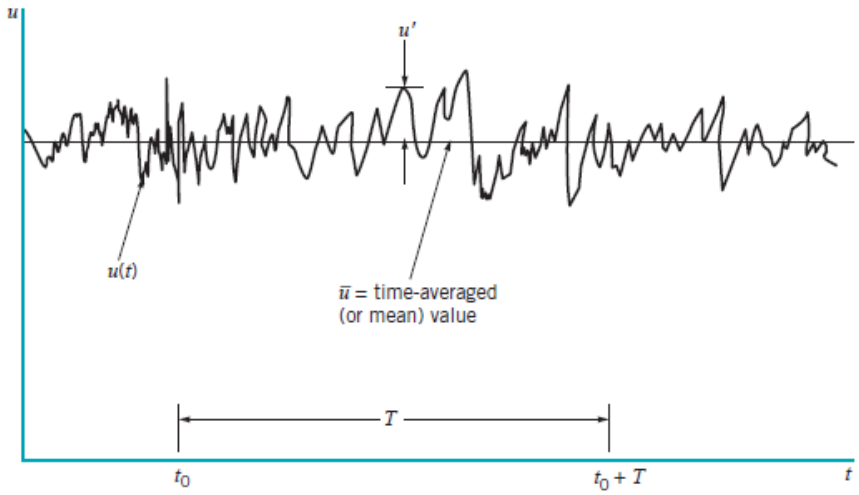

Figure 5.11. The time-averaged, $\overline{u}$,and fluctuating, u' , description of a parameter for turbulent flow

Turbulent flow shear stress is larger than laminar flow shear stress because of the irregular, random motion. The *total shear stress* in turbulent flow can be expressed as

$$\tau = \mu \frac{d\bar{u}}{dy} - \rho\overline{u'v'} = \tau_{\text{lam}} + \tau_{\text{turb}}$$

Note that if the flow is laminar $u' = v' = 0$, so that $\overline{u'v'} = 0$ and the above equation reduces o the customary random molecule-motion induced laminar shear stress, $\tau_{lam} = \mu d\bar{u}/\text{dy}$. For turbulent flow it is found that the turbulent shear stress, $\tau_{turb} = -\rho\overline{u'v'}$ is positive. Hence, the shear stress is greater in turbulent flow than in laminar flow.

Considerable information concerning turbulent velocity profiles has been obtained through the use of dimensional analysis, experimentation, numerical simulations, and semiempirical theoretical efforts. As is indicated in Fig.5.12, fully developed turbulent flow in a pipe can be broken into three regions which are characterized by their distances from the wall: the viscous sublayer very near the pipe wall, the overlap region, and the outer turbulent layer throughout the center portion of the flow.

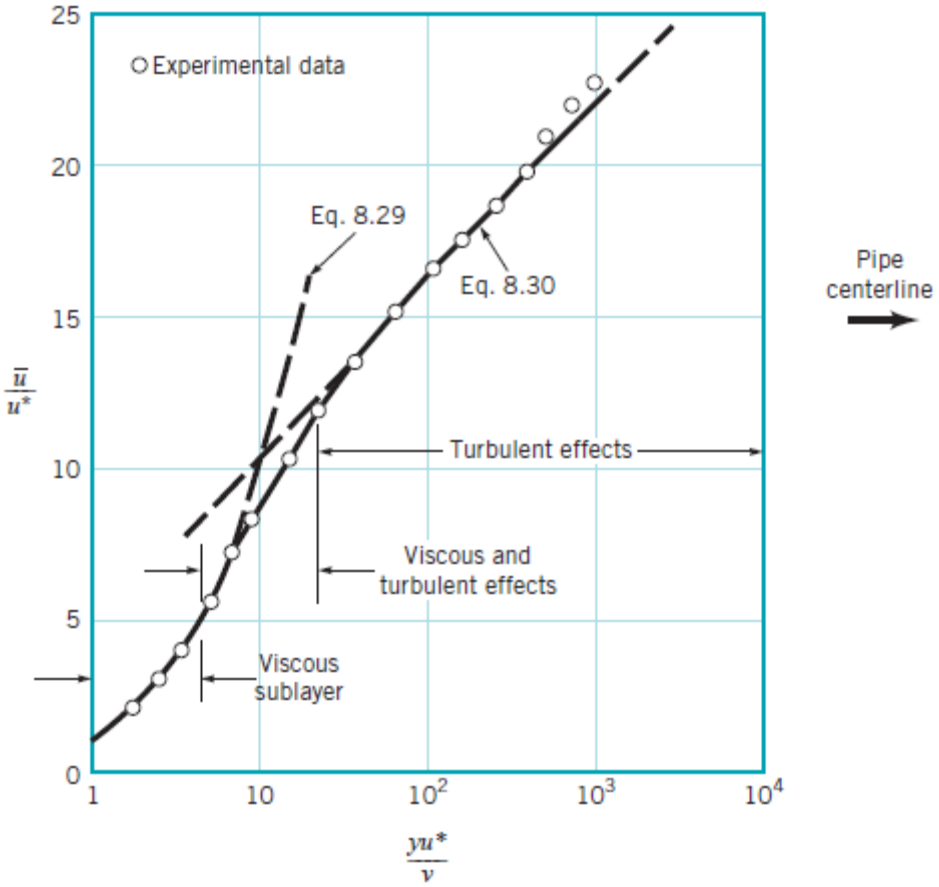

Figure 5.12. Typical structure of the turbulent velocity profile in a pipe

Within the viscous sublayer the viscous shear stress is dominant compared with the turbulent (or Reynolds) stress, and the random, eddying nature of the flow is essentially absent. In the outer turbulent layer the Reynolds stress is dominant, and there is considerable mixing and randomness to the flow. The character of the flow within these two regions is entirely different. For example, within the viscous sublayer the fluid viscosity is an important parameter; the density is unimportant. In the outer layer the opposite is true. By a careful use of dimensional analysis arguments for the flow in each layer and by a matching of the results in the common overlap layer, it has been possible to obtain the following conclusions about the turbulent velocity profile in a smooth pipe. In the viscous sublayer the velocity profile can be written in dimensionless form as

$$\frac{\bar{u}}{u^*} = \frac{yu^*}{\nu}$$

Where y=R-r is the distance measured from the wall, $\bar{u}$ is the time-averaged x component of velocity, and $u^* = (\frac{\tau_w}{\rho})^{1/2}$ is termed ***the friction velocity***. Note that u^* is not an actual velocity of the fluid-it is merely a quantity that has dimensions of velocity.

This equation is known as the ***law of the wall,*** and it is found to satisfactorily correlate with experimental data for smooth surfaces for $0 \leq yu^*/\nu \leq 5$. The viscous sublayer is usually quite thin. For viscous sublayer can be calculated by

$$0 \leq yu^*/\nu \leq 5$$

Thus, thickness of viscous sublayer: $y = \delta_{sublayer} = \frac{5\nu}{u^*}$ This is valid very near the smooth wall. We conclude that *the thickness of the viscous sublayer is proportional to the kinematic viscosity and inversely proportional to the average flow velocity*. In other words, the viscous sublayer is suppressed and it gets thinner as the velocity (and thus the Reynolds number) increases. Consequently, the velocity profile becomes nearly flat and thus the velocity distribution becomes more uniform at very high Reynolds numbers. The quantity ν/*u** has dimensions of length and is called the ***viscous length;*** it is used to nondimensionalize the distance *y* from the surface.

Dimensional analysis arguments indicate that in the overlap region the velocity should vary as the logarithm of *y*. Thus, the following expression has been proposed:

$$\frac{\overline{u}}{u^*} = 2.5 \ln\left(\frac{yu^*}{\nu}\right) + 5.0$$

Where the constants 2.5 and 5.0 have been determined experimentally. As is indicated in the above Fig.5.12, for regions not too close to the smooth wall, but not all the way out to the pipe center, The last equation gives a reasonable correlation with the experimental data. Note that the horizontal scale is a logarithmic scale. This tends to exaggerate the size of the viscous sublayer relative to the remainder of the flow. The viscous sublayer is usually quite thin. Similar results can be obtained for turbulent flow past rough walls (5.13).

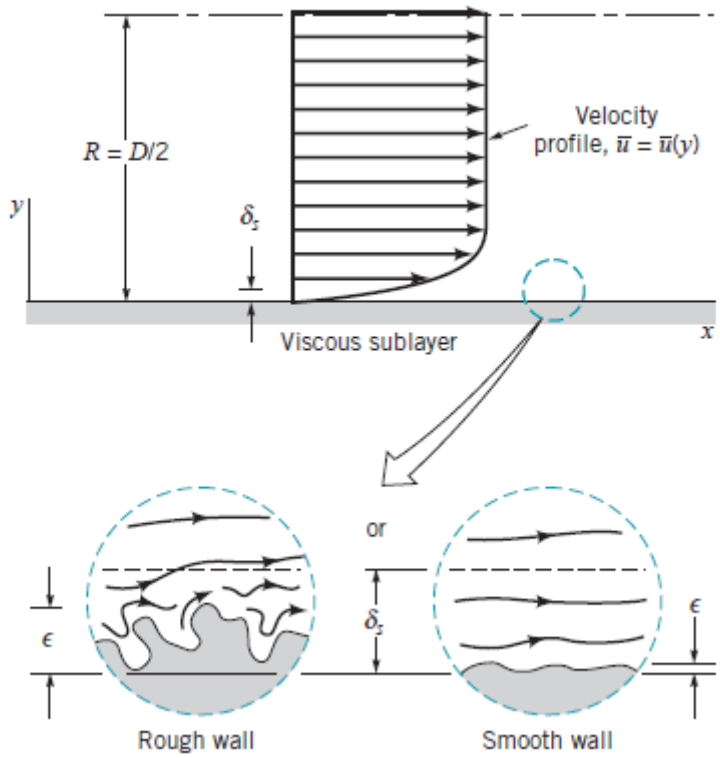

Figure 5.13. Flow in the viscous sublayer near rough and smooth walls.

A number of other correlations exist for the velocity profile in turbulent pipe flow. In the central region (the outer turbulent layer) the expression

$$\frac{V_c - \bar{u}}{u^*} = 2.5 \ln(\frac{R}{y})$$

Where; V_c is the centerline velocity, is often suggested as a good correlation with experimental data. Another often-used (and relatively easy to use) correlation is the empirical *power-law velocity profile*

$$\frac{\bar{u}}{V_c} = \left(1 - \frac{r}{R}\right)^{1/n}$$

In this representation, the value of n is a function of the Reynolds number, as is indicated in below Fig.5.14.

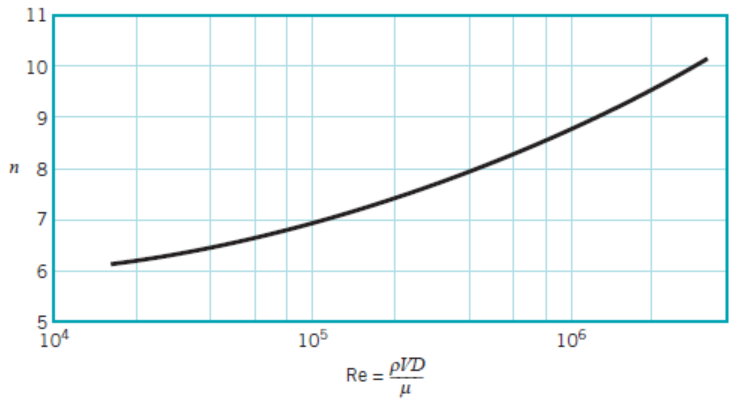

Figure 5.14. Exponent, *n*, for power-law velocity profiles.

The one-seventh power-law velocity profile (n=7) is often used as a reasonable approximation for many practical flows. Typical turbulent velocity profiles based on this power-law representation are shown in the below Fig.5.15.

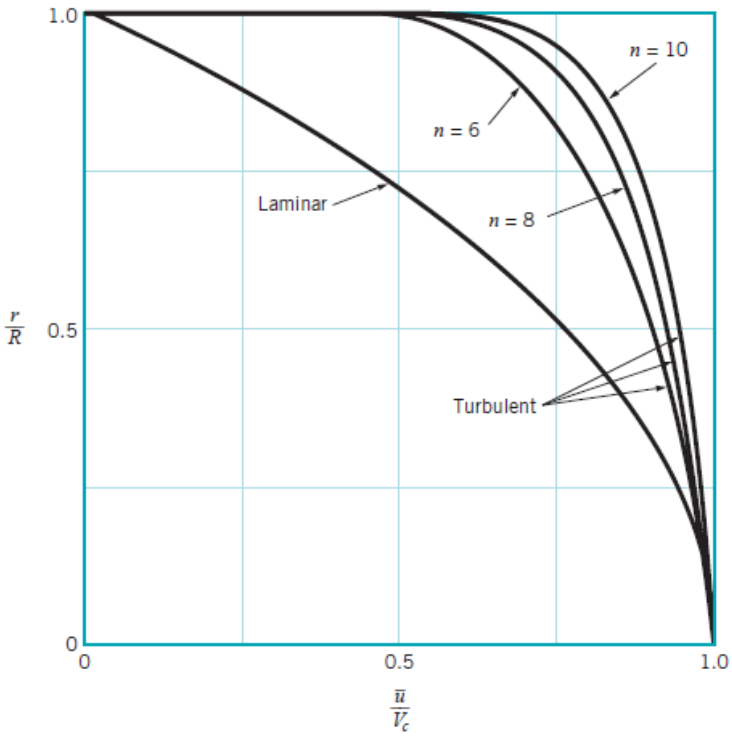

Figure 5.15. Typical laminar flow and turbulent flow velocity profiles.

Pressure Drop and Head Loss

The overall head loss for the pipe system consists of the head loss due to viscous effects in the straight pipes, termed the ***major loss*** and denoted, h_{Lmajor}, and the head loss in the various pipe components, termed the ***minor loss*** and denoted, h_{Lminor}. That is, $h_L = h_{Lmajor} + h_{Lminor}$

The head loss designations of "major" and "minor" do not necessarily reflect the relative importance of each type of loss. For a pipe system that contains many components and a relatively short length of pipe, the minor loss may actually be larger than the major loss.

$$h_{Lmajor} = f\frac{L}{D}\frac{V^2}{2g}$$

This equation called the *Darcy–Weisbach equation*, is valid for any fully developed, steady, incompressible pipe flow—whether the pipe is horizontal or on a hill. The friction factor (f) in fully developed turbulent pipe flow depends on the ***Reynolds number*** ($Re = \rho VD/\mu$) and ***the relative roughness,*** ε/*D*, which is the ratio of the mean height of roughness of the pipe to the pipe diameter and are not present in the laminar formulation because the two parameters ρ and ε are not important in fully developed laminar pipe flow. Typical roughness values for various pipe surfaces are given in Table 5.2.

Table 5.2. Rougness for new pipes

Equivalent Roughness for New Pipes [From Moody (Ref. 7) and Colebrook (Ref. 8)]

	Equivalent Roughness, ε
Pipe	**Millimeters**
Riveted steel	0.9–9.0
Concrete	0.3–3.0
Wood stave	0.18–0.9
Cast iron	0.26
Galvanized iron	0.15
Commercial steel or wrought iron	0.045
Drawn tubing	0.0015
Plastic, glass	0.0 (smooth)

The below figure shows the functional dependence of *f* on Re and *ε/D* and is called the ***Moody chart*** in honor of L. F. Moody, who, along with C. F. Colebrook, correlated the original data of Nikuradse in terms of the relative roughness of commercially available pipe materials. It should be noted that the values of *ε/D* do not necessarily correspond to the actual values obtained by a microscopic determination of the average height of the roughness of the surface (Fig 16). They do, however, provide the correct correlation for $f = \emptyset(Re, \frac{\varepsilon}{D})$.

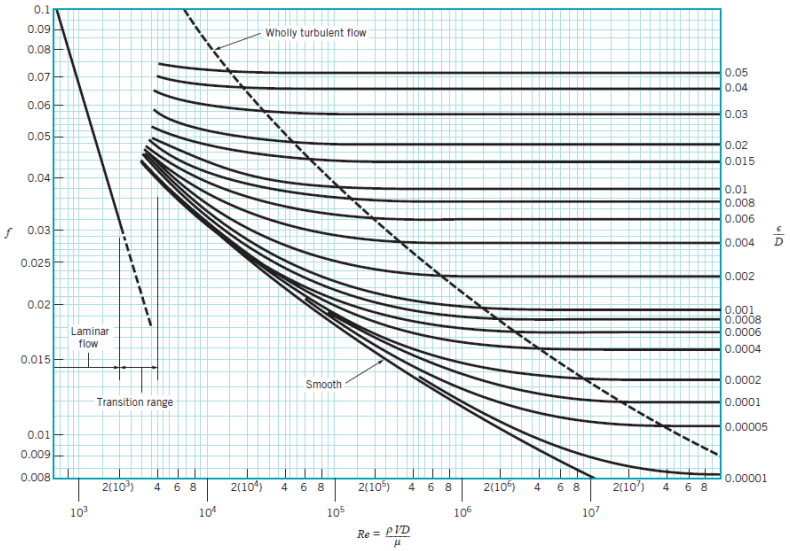

Figure 5.16. Friction factor as a function of Reynolds number and relative roughness for round pipes-the Moody chart.

Note that even for smooth pipes $(\varepsilon = 0)$ the friction factor is not zero. That is, there is a head loss in any pipe, no matter how smooth the surface is made. This is a result of the no-slip boundary condition that requires any fluid to stick to any solid surface it flows over. There is always some microscopic surface roughness that produces the no-slip behavior (and thus) on the molecular level, even when the roughness is considerably less than the viscous sublayer thickness. Such pipes are called *hydraulically smooth*.

The Moody chart covers an extremely wide range in flow parameters. The Moody chart, on the other hand, is universally valid for all steady, fully developed, incompressible pipe flows. The following equation from Colebrook is valid for the entire nonlaminar range of the Moody chart

$$\frac{1}{\sqrt{f}} = -2.0 \log\left(\frac{\varepsilon/D}{3.7} + \frac{2.51}{\mathrm{Re}\sqrt{f}}\right)$$

In fact, the Moody chart is a graphical representation of this equation, which is an empirical fit of the pipe flow pressure drop data. The above Equation is called the ***Colebrook formula.*** A difficulty with its use is that it is implicit in the dependence of *f*. That is, for given conditions (Re and ε/D), it is not possible to solve for *f* without some sort of iterative scheme. With the use of modern computers and calculators, such calculations are not difficult. A word of caution is in order concerning the use of the Moody chart or the equivalent Colebrook formula. Because of various inherent inaccuracies involved (uncertainty in the relative roughness, uncertainty in the experimental data used to produce the Moody chart, etc.), the use of several place accuracy in pipe flow problems is usually not justified. As a rule of thumb, a 10% accuracy is the best expected. It is possible to obtain an equation that adequately approximates the Colebrook_Moody chart

relationship but does not require an iterative scheme. For example, an alternate form, which is easier to use, is given by by S. E. Haaland in 1983 as

$$\frac{1}{\sqrt{f}} = -1.8 \log\left[\left(\frac{\varepsilon/D}{3.7}\right)^{1.11} + \frac{6.9}{\mathrm{Re}}\right]$$

Where one can solve for *f* explicitly. The results obtained from this relation are within 2 percent of those obtained from the Colebrook equation

To avoid tedious iterations in head loss, flow rate, and diameter calculations, Swamee and Jain proposed the following explicit relations in 1976 that are accurate to within 2 percent of the Moody chart

for $10^{-6} < \frac{\varepsilon}{D} < 10^{-2}$ *and* $3000 < Re < 3\times10^{8}$

$$h_L = 1.07\frac{Q^2 L}{gD^5}\left\{ln\left[\frac{\varepsilon}{3.7D} + 4.62\,(\frac{\nu D}{Q})^{0.9}\right]\right\}^{-2}$$

for $Re > 2000$ $$Q = -0.965(\frac{gD^5 h_L}{L})^{0.5}\, ln\left[\frac{\varepsilon}{3.7D} + (\frac{3.17\nu^2 L}{gD^3 h_L})^2\right]$$

for $10^{-6} < \frac{\varepsilon}{D} < 10^{-2}$ and $5000 < Re < 3\times10^{8}$

$$D = 0.66\left[\varepsilon^{1.25}\,(\frac{LQ^2}{gh_L})^{4.75} + \nu Q^{9.4}(\frac{L}{gh_L})^{5.2}\right]^{0.04}$$

If $Re \leq 10^5$ and the pipe is hydraulically smooth (ε=0), we can take $f=0.316/Re^{0.25}$.

Note that all quantities are dimensional and the units simplify to the desired unit (for example, to m or ft in the last relation) when consistent units are used. Noting that the Moody chart is accurate to within 15 percent of experimental data, we should have no reservation in using these approximate relations in the design of piping systems.

As discussed in the above section, the head loss in long, straight sections of pipe, the major losses, can be calculated by use of the friction factor obtained from either the Moody chart or the Colebrook equation. Most pipe systems, however, consist of considerably more than straight pipes. These additional components (valves, bends, tees, and the like) add to the overall head loss of the system. Such losses are generally termed *minor losses*, h_{Lminor}, with the corresponding head loss

denoted In this section we indicate how to determine the various minor losses that commonly occur in pipe systems.

The friction loses for noncircular pipes can be calculated by *Darcy–Weisbach equation*. But The Reynolds number for flow in these pipes is based on the hydraulic diameter $D_h=4R=4Ac/p$, where ***R*** is the ***hydraulic radius*** **(**Hydraulic radius is defined as the ratio of the channel's cross-sectional area of the flow to its ***wetted perimeter*****).** *Ac* is the cross-sectional area of the flow and *p* is its wetted perimeter (the length of the perimeter of the cross section in contact with the fluid).

$$R = \frac{A_c}{p} \qquad D_h = 4\frac{A_c}{p} \qquad Re = \frac{4RV}{\nu} = \frac{D_h V}{\nu}$$

The relative rougness is ε/4R.

$$h_{Lmajor} = f\frac{L}{D_h}\frac{V^2}{2g}$$

Example: The water is fully flowing through a duct that has a=25 cm and b=10 cm. Determine hydraulic radius of the duct. If water is filled up to half of the pipe. What is hydraulic radius?

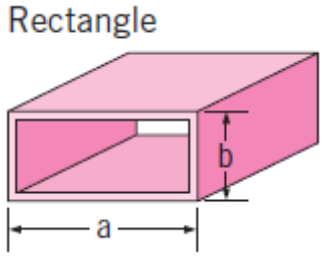

Solution: If the duct is full of water.

$$R = \frac{A_c}{p} = \frac{0.25\times0.10}{2(0.25+0.10)} = 0.036\,m$$

If water is filled up to half of the pipe:

$$R = \frac{A_c}{p} = \frac{0.25\times0.10/2}{2(0.25+0.10/2)} = 0.018\,m$$

The head loss associated with flow through a valve is a common minor loss. The purpose of a valve is to provide a means to regulate the flowrate. This is accomplished by changing the geometry of the system (i.e., closing or opening

the valve alters the flow pattern through the valve), which in turn alters the losses associated with the flow through the valve. The flow resistance or head loss through the valve may be a significant portion of the resistance in the system. In fact, with the valve closed, the resistance to the flow is infinite—the fluid cannot flow. Such minör losses may be very important indeed. With the valve wide open the extra resistance due to the presence of the valve may or may not be negligible.

The flow pattern through a typical component such as a valve is shown in Fig.5.17. It is not difficult to realize that a theoretical analysis to predict the details of such flows to obtain the head loss for these components is not, as yet, possible. Thus, the head loss information for essentially all components is given in dimensionless form and based on experimental data. The most common method used to determine these head losses or pressure drops is to specify the ***loss coefficient,*** $\mathbf{K_L}$**.**

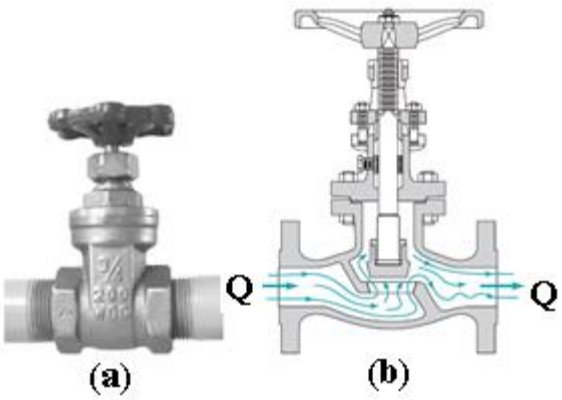

Figure 5.17. Flow through a valve. Losses due to pipe

Minor losses are usually expressed in terms of the **loss coefficient** K_L (Fig 5.18, 5.19, 5.20 and 5.21) (also called the **resistance coefficient**), defined as

$$h_{Lminor} = K_L \frac{V^2}{2g}$$

where h_L is the *additional* irreversible head loss in the piping system caused by insertion of the component, and is defined as $h_L = \Delta P_L / \rho g$. The pressure drop across a component that has a loss coefficient of is equal to the dynamic pressure, $\rho V^2/2$.

Minor losses are sometimes given in terms of an *equivalent length*, l_{eq} . In this terminology, the head loss through a component is given in terms of the equivalent length of pipe that would produce the same head loss as the component. That is,

$$l_{eq} = K_L \frac{D}{f}$$

where D and f are based on the pipe containing the component. The head loss of the pipe system is the same as that produced in a straight pipe whose length is equal to the pipes of the original system plus the sum of the additional equivalent lengths of all of the components of the system. Most pipe flow analyses, including those in this book, use the loss coefficient method rather than the equivalent length method to determine the minor losses.

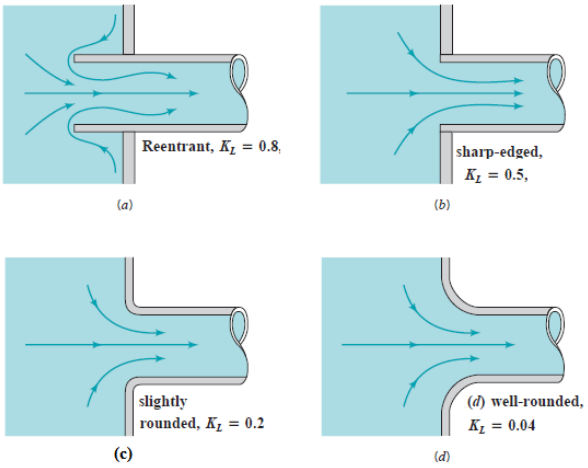

Figure 5.18. Entrance flow conditions and loss coefficient

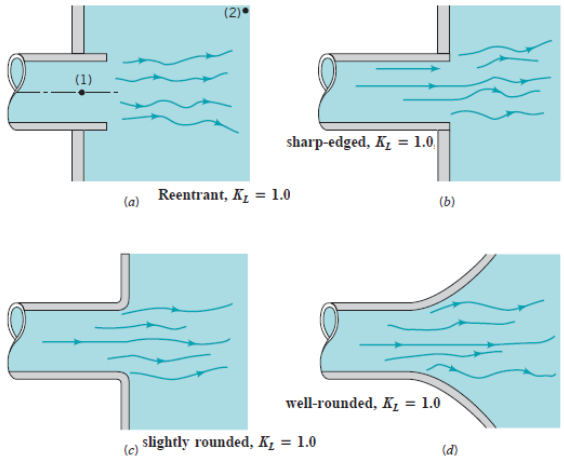

Figure 5.19. Exit flow conditions and loss coefficient.

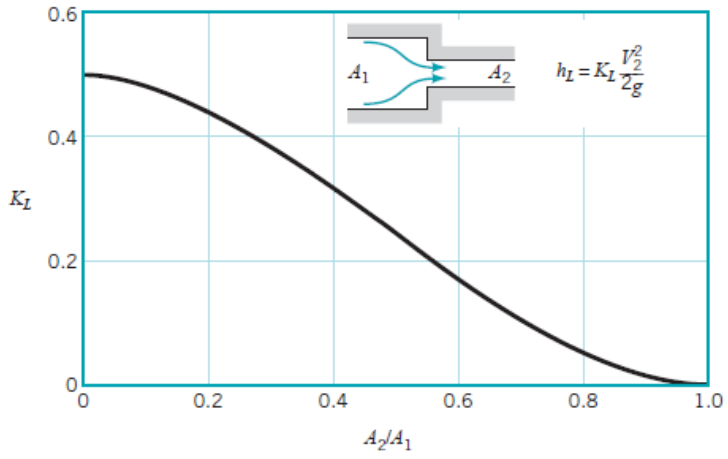

Figure 5.20. Loss coefficient for a sudden contraction

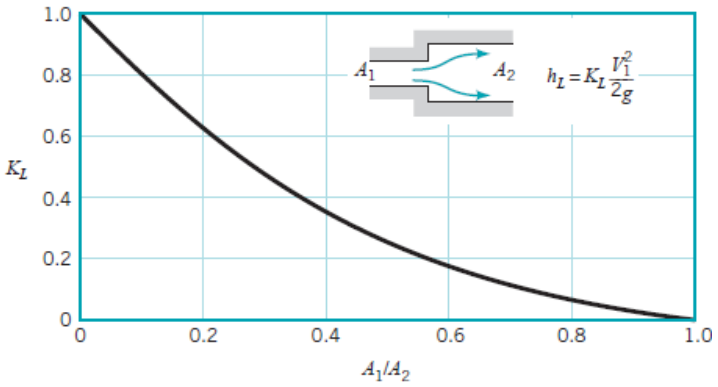

Figure 5.21. Loss coefficient for a sudden expansion

The total head loss in a piping system is determined from $h_L = h_{Lmajor} + h_{Lminor}$

$$h_L = \boldsymbol{f}\frac{\boldsymbol{L}}{\boldsymbol{D}}\frac{\boldsymbol{V^2}}{\boldsymbol{2g}} + K_L\frac{V^2}{2g}$$

Once the useful pump head is known, the *mechanical power that needs to be delivered by the pump to the fluid* and the *electric power consumed by the motor of the pump* for a specified flow rate are determined from

$$\dot{W}_p = \frac{\rho g Q h_L}{\eta_p} \text{ for pump}$$

$$\dot{W}_e = \frac{\rho g Q h_L}{\eta_p \eta_m} \text{ for electrik motor}$$

Where; η_p is the efficiency of the pump. $\eta_m$is the efficiency of the motor.

5.4. Pipe Flowrate Measurement

It is often necessary to determine experimentally the flowrate in a pipe. In before chapter we introduced various types of flow-measuring devices (venturi meter, nozzle meter, orifice meter, etc.) and discussed their operation under the assumption that viscous effects were not important. In this section we will indicate how to account for the ever-present viscous effects in these flow meters. We will also indicate other types of commonly used flow meters. Orifice, nozzle and Venturi meters involve the concept "high velocity gives low pressure."

5.4.1 Pipe Flowrate Meters

Three of the most common devices used to measure the instantaneous flowrate in pipes are *the orifice meter, the nozzle meter, and the venturi meter.* Each of these

meters operates on the principle that a decrease in flow area in a pipe causes an increase in velocity that is accompanied by a decrease in pressure. Correlation of the pressure difference with the velocity provides a means of measuring the flowrate. In the absence of viscous effects and under the assumption of a horizontal pipe, application of the Bernoulli equation between points (1) and (2) shown in Fig.5.22 gave

$$Q_{\text{ideal}} = A_2 V_2 = A_2 \sqrt{\frac{2(p_1 - p_2)}{\rho(1 - \beta^4)}}$$

Where; $\beta = \frac{D_2}{D_1}$. Based on the results of the previous sections of this chapter, we anticipate that there is a head loss between (1) and (2) so that the governing equations become

$$Q = A_1 V_1 = A_2 V_2$$

$$\frac{p_1}{\gamma} + \frac{V_1^2}{2g} = \frac{p_2}{\gamma} + \frac{V_2^2}{2g} + h_L$$

The ideal situation has h_L=0 and results in above equation. The difficulty in including the head loss is that there is no accurate expression for it. The net result is that empirical coefficients are used in the flowrate equations to account for the complex real-world effects brought on by the nonzero viscosity. The coefficients are discussed in this section.

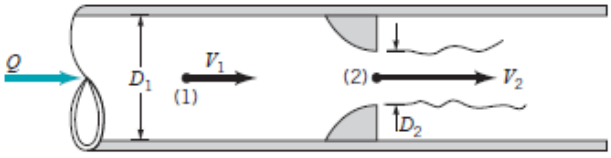

Figure 5.22. Typical pipe flow meter geometry.

A typical ***orifice meter*** is constructed by inserting between two flanges of a pipe a flat plate with a hole, as shown in the below Fig.5.23.

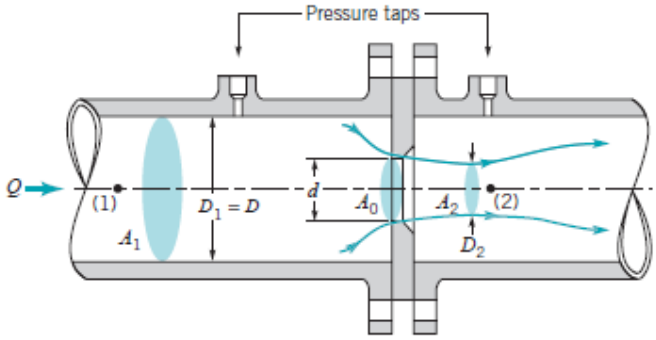

Figure 5.23. Typical orifice meter construction.

The pressure at point (2) within the vena contracta is less than that at point (1). Nonideal effects occur for two reasons. First, the vena contracta area, A_2 is less than the area of the hole, A_0, by an unknown amount. Thus, $A_2=C_cA_0$, where C_c is the contraction coefficient (Cc<1). Second, the swirling flow and turbulent motion near the orifice plate introduce a head loss that cannot be calculated theoretically. Thus, an *orifice discharge coefficient, C_0,* is used to take these effects into account. That is,

$$Q = C_o Q_{\text{ideal}} = C_o A_o \sqrt{\frac{2(p_1 - p_2)}{\rho(1 - \beta^4)}}$$

Where; $A_0 = \frac{\pi d^2}{4}$ is the area of the hole in the orifice plate. The value of C_0 is a function of $\beta = \frac{d}{D}$ and the Reynolds number $Re = \rho VD/\mu$, where $V = \frac{Q}{A_1}$. Typical values of C_0 are given in the below Fig. 5.24. The experimentally determined data for orifice discharge coefficient for $0.25 < \beta < 0.75$ *and* $10^4 < Re < 10^7$ is expressed as

$$\text{Orifice meters:} \quad C_0 = 0.5959 + 0.0312\beta^{2.1} - 0.184\beta^8 + \frac{91.71\beta^{2.5}}{\text{Re}^{0.75}}$$

For flows with high Reynolds numbers (Re ≥ 30.000), the value of C_0 can be taken to be $\boldsymbol{C_0=0.61}$ for orifices.

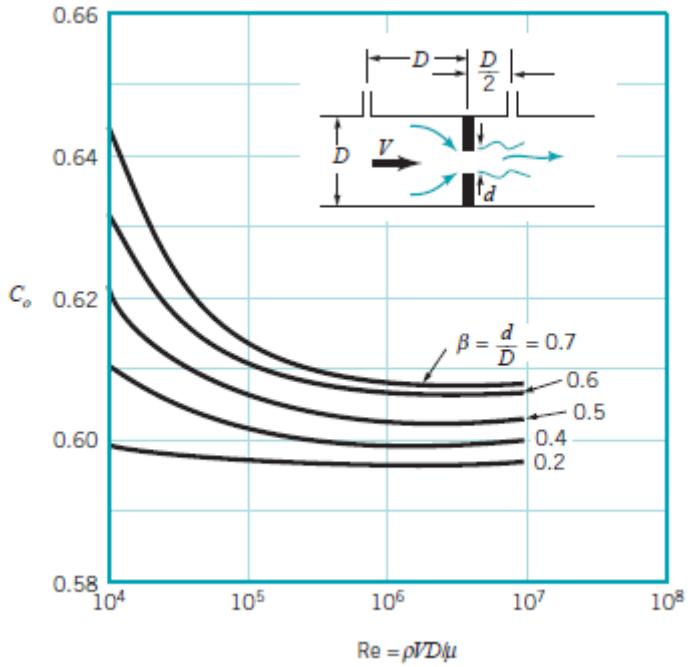

Figure 5.24. Orifice meter discharge coefficient

For a given value of C_0, the flowrate is proportional to the square root of the pressure diffrence. Note that the value of C_0 depends on the specific construction of the orifice meter (i.e., the placement of the pressure taps, whether the orifice plate edge is square or beveled, etc.). Very precise conditions governing the construction of standard orifice meters have been established to provide the greatest accuracy possible.

Another type of pipe flow meter that is based on the same principles used in the orifice meter is the ***nozzle meter,*** three variations of which are shown in the below Fig.5.25.

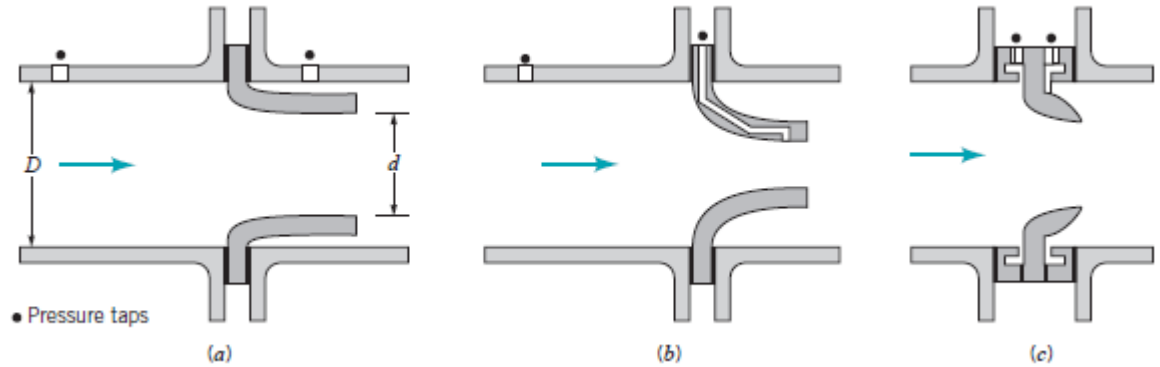

Figure 5.25. Typical nozzle meter construction.

This device uses a contoured nozzle (typically placed between flanges of pipe sections) rather than a simple (and less expensive) plate with a hole as in an orifice

meter. The resulting flow pattern for the nozzle meter is closer to ideal than the orifice meter flow. There is only a slight vena contracta and the secondary flow separation is less severe, but there still are viscous effects. These are accounted for by use of the ***nozzle discharge coefficient***, C_n, where

$$Q = C_n Q_{ideal} = C_n A_n \sqrt{\frac{2(p_1 - p_2)}{\rho(1 - \beta^4)}}$$

With $A_n = \frac{\pi d^2}{4}$. As with the orifice meter, the value of C_n is a function of the diameter rato, with $A_n = \frac{\pi d^2}{4}$. And the Reynolds number, $Re = \frac{\rho VD}{\mu}$. Typical values obtained from experiments are shown in the below Fig.5.26. Again, precise values of C_n depend on the specific details of the nozzle design. Note that $C_n > C_0$ the nozzle meter is more efficient (less energy dissipated) than the orifice meter. C_n for $0.25 < \beta < 0.75$ *and* $10^4 < Re < 10^7$ can be calculated from the following equation.

$$\mathbf{C_n} = 0.9975 - \frac{6.53\beta^{0.5}}{\mathrm{Re}^{0.5}}$$

For flows with high Reynolds numbers (Re≥ 30.000), the value of C_n can be taken to be ***C_n=0.96*** for flow nozzles.

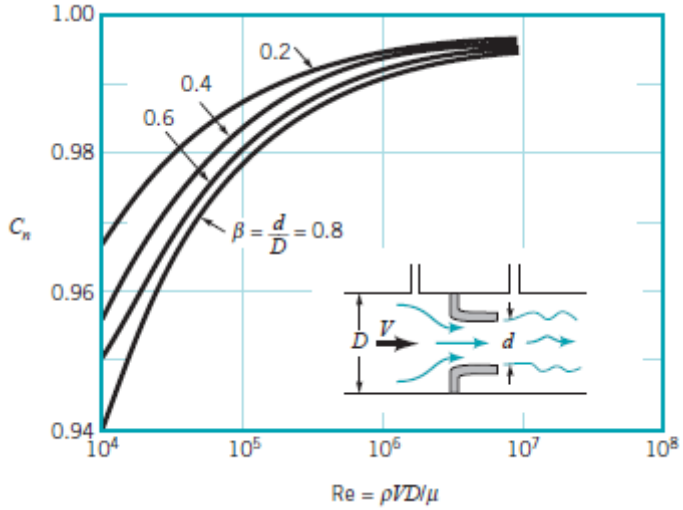

Figure 5.26. Nozzle meter discharge coefficient

The most precise and most expensive of the three obstruction-type flow meters is the ***Venturimeter*** shown in Fig.5.27.

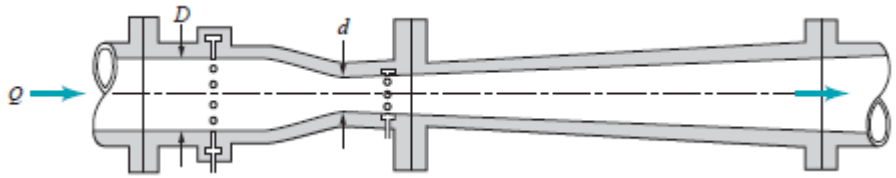

Figure 5.27. Typical venturi meter construction.

Although the operating principle for this device is the same as for the orifice or nozzle meters, the geometry of the venturi meter is designed to reduce head losses to a minimum. This is accomplished by providing a relatively streamlined contraction (which eliminates separation ahead of the throat) and a very gradual expansion downstream of the throat (which eliminates separation in this decelerating portion of the device). Most of the head loss that occurs in a well-designed venturi meter is due to friction losses along the walls rather than losses associated with separated flows and the inefficient mixing motion that accompanies such flow. Thus, the flowrate through a Venturi meter is given by

$$Q = C_v Q_{\text{ideal}} = C A_T \sqrt{\frac{2(p_1 - p_2)}{\rho(1 - \beta^4)}}$$

Where; $A_T = \frac{\pi d^2}{4}$ is the throat area. The range of values of Cv, the Venturi discharge coefficient, is given in the following Fig. 5.28.

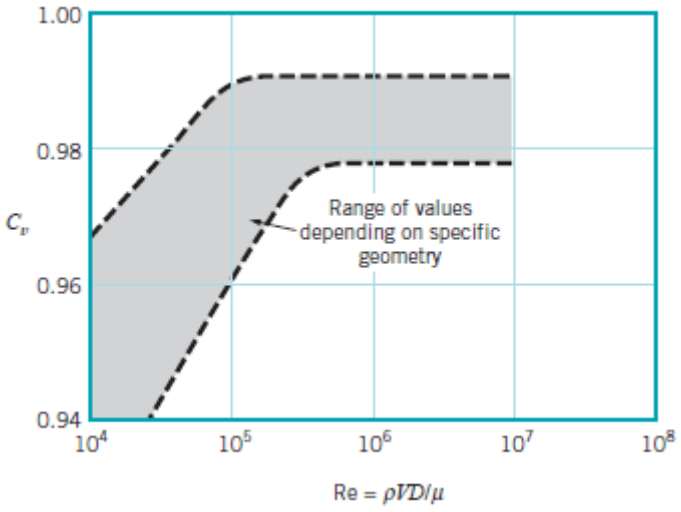

Figure 5.28. Venturi meter discharge coefficient.

The throat-to-pipe diameter ratio $\left(\beta = \frac{d}{D}\right)$, the Reynolds number, and the shape of the converging and diverging sections of the meter are among the parameters that affect the value of C_v.

Owing to its streamlined design, the discharge coefficients of Venturi meters are very high, ranging between 0.95 and 0.99 (the higher values are for the higher Reynolds numbers) for most flows. In the absence of specific data, we can take ***Cv*=0.98** for Venturi meters. Also, the Reynolds number depends on the flow velocity, which is not known a priori. Therefore, the solution is iterative in nature when curve-fit correlations are used for *Cv*.

5.5. Chapter Summary and Study Guide

This chapter discussed the flow of a viscous fluid in a pipe. General characteristics of laminar, turbulent, fully developed, and entrance flows are considered. Poiseuille's equation is obtained to describe the relationship among the various parameters for fully developed laminar flow.

Some of the important equations in this chapter are given below.

Entrance length

$$\frac{\ell_e}{D} = 0.06\ \text{Re for laminar flow}$$

$$\frac{\ell_e}{D} = 4.4\ (\text{Re})^{1/6} \text{ for turbulent flow}$$

Pressure drop for fully developed laminar pipe flow

$$\Delta p = \frac{4\ell\tau_w}{D}$$

Velocity profile for fully developed laminar pipe flow

$$u(r) = \left(\frac{\Delta p D^2}{16\mu\ell}\right)\left[1 - \left(\frac{2r}{D}\right)^2\right] = V_c\left[1 - \left(\frac{2r}{D}\right)^2\right]$$

Volume flowrate for fully developed laminar pipe flow

$$Q = \frac{\pi D^4\, \Delta p}{128\mu\ell}$$

Friction factor for fully developed laminar pipe flow

$$f = \frac{64}{\text{Re}}$$

Pressure drop for a horizontal pipe

$$\Delta p = f\frac{\ell}{D}\frac{\rho V^2}{2}$$

Head loss due to major losses

$$h_{L\,\text{major}} = f\frac{\ell}{D}\frac{V^2}{2g}$$

Colebrook formula

$$\frac{1}{\sqrt{f}} = -2.0\log\left(\frac{\varepsilon/\text{D}}{3.7} + \frac{2.51}{\text{Re}\sqrt{f}}\right)$$

Explicit alternative to Colebrook formula

$$\frac{1}{\sqrt{f}} = -1.8 \log\left[\left(\frac{\varepsilon/D}{3.7}\right)^{1.11} + \frac{6.9}{Re}\right]$$

Head loss due to minor losses

$$h_{L\,minor} = K_L \frac{V^2}{2g}$$

Volume flowrate for orifice, nozzle, or Venturi meter

$$Q = C_i A_i \sqrt{\frac{2(p_1 - p_2)}{\rho(1 - \beta^4)}}$$

The design and analysis of piping systems involve the determination of the head loss, flow rate, or the pipe diameter. Tedious iterations in these calculations can be avoided by the approximate Swamee–Jain formulas expressed as

for $10^{-6} < \frac{\varepsilon}{D} < 10^{-2}$ *and* $3000 < Re < 3\times10^{8}$

$$h_L = 1.07 \frac{Q^2 L}{gD^5}\left\{ln\left[\frac{\varepsilon}{3.7D} + 4.62\,(\frac{\nu D}{Q})^{0.9}\right]\right\}^{-2}$$

for $Re > 2000$

$$Q = -0.965(\frac{gD^5 h_L}{L})^{0.5}\, ln\left[\frac{\varepsilon}{3.7D} + (\frac{3.17\nu^2 L}{gD^3 h_L})^2\right]$$

for $10^{-6} < \frac{\varepsilon}{D} < 10^{-2}$ and $5000 < Re < 3\times10^{8}$

$$D = 0.66\left[\varepsilon^{1.25}\,(\frac{LQ^2}{gh_L})^{4.75} + \nu Q^{9.4}(\frac{L}{gh_L})^{5.2}\right]^{0.04}$$